



King Saud University
Arabian Journal of Chemistry

www.ksu.edu.sa
www.sciencedirect.com



ORIGINAL ARTICLE

Effects of aniline concentrations on the electrical and mechanical properties of polyaniline polyvinyl alcohol blends

J. Bhadra ¹, N.J. Al-Thani ^{*}, N.K. Madi ¹, M.A. Al-Maadeed ¹

Centre for Advanced Materials, Qatar University, Qatar

Received 20 January 2015; accepted 18 April 2015

KEYWORDS

Polyaniline;
Polyvinyl alcohol;
Composite;
Conductivity;
Tensile strength

Abstract In this work, we present an exclusive study on the effect of the feeding ratio of the monomer (aniline) on the structural, thermal, mechanical and electrical properties of polyaniline (PANI) polyvinyl alcohol (PVA) blends. The films obtained from the blends are characterised to determine their surface properties and structural morphology (elemental analysis, SEM and FTIR), thermal properties (TGA and DSC) and optical properties (UV–Vis spectroscopy). We study the effects of aniline on the mechanical and electrical properties of the composites by performing tensile, four probe and A.C. conductivity measurements, respectively. The SEM images reveal a heterogeneous distribution of conductive PANI particles in the continuous PVA matrix. During this experiment, the tensile strength of the blend films is maintained with an increase in the amount of aniline (up to 25 wt%), and this behaviour is attributed to intermolecular hydrogen bonding between PANI and PVA in the presence of the surfactant DBSA. The potential attraction of the experiment lies in the nature of the conductivity (of the blend films), which is found to increase from 10^{-8} to 10^{-3} S/cm with a percolation threshold of 0.78 wt%.

© 2015 Production and hosting by Elsevier B.V. on behalf of King Saud University. This is an open access article under the CC BY-NC-ND license (<http://creativecommons.org/licenses/by-nc-nd/4.0/>).

1. Introduction

In recent years, the conducting polymer polyaniline (PANI) has gained a considerable amount of attention from researchers worldwide due to its high environmental stability, ease of preparation, tuneable electrical properties, and low cost. However, the utilisation of PANI has been limited because of its poor solubility, fusibility, mechanical properties, and processability. To overcome these disadvantages (i.e., to increase its processability), a number of methods have been studied. The possibility of processing PANI in the form of blends with commercial polymers (Kim et al., 2005; Zareh

* Corresponding author. Tel.: +974 4033 5666; fax: +974 4033 3989.

E-mail addresses: jollybhadra@qu.edu.qa (J. Bhadra), n.al-thani@qu.edu.qa (N.J. Al-Thani), nmadi@qu.edu.qa (N.K. Madi), m.alali@qu.edu.qa (M.A. Al-Maadeed).

¹ Tel.: +974 4033 5666; fax: +974 4033 3989.

Peer review under responsibility of King Saud University.



Production and hosting by Elsevier

<http://dx.doi.org/10.1016/j.arabjc.2015.04.017>

1878-5352 © 2015 Production and hosting by Elsevier B.V. on behalf of King Saud University.

This is an open access article under the CC BY-NC-ND license (<http://creativecommons.org/licenses/by-nc-nd/4.0/>).

Please cite this article in press as: Bhadra, J. et al., Effects of aniline concentrations on the electrical and mechanical properties of polyaniline polyvinyl alcohol blends. Arabian Journal of Chemistry (2015), <http://dx.doi.org/10.1016/j.arabjc.2015.04.017>

et al., 2011; Malmongea et al., 2010; Yuxi and Rutledge, 2012) has opened a wide range of potential applications and increased the technological potential of these materials. In addition to these methods, the most widely adopted strategy is to dope PANI with organic acids possessing long alkyl-chain sulphonic acids (camphorsulphonic acid (CSA), dodecylbenzene sulphonic acid (DBSA), etc. (Wu and Zhang, 2013; Bhadra et al., 2014). In fact, blends of PANI doped with camphorsulphonic acid (PANI-CSA) in solution with polar polymer matrixes, such as poly(methyl methacrylate) (PMMA) (Araujo et al., 2007) and polyamide (PA) (Hopkins et al., 2011), and PANI doped with DBSA (PANI-DBSA) in solution with polystyrene (PS) (Castillo-Castro et al., 2007), polyvinyl chloride (PVC) (Afzal et al., 2010) and polyvinyl alcohol (PVA) (Bhadra et al., 2014; Han et al., 2002) have been reported. Because of outstanding water solubility and processability, PVA is very useful in a number of applications (Thekkayil et al., 2014; Morita, 1994; Pawar and Purwar, 2013). The PANI composite is found to be uniformly embedded in this insulating polymer matrix of PVA (Bhadra et al., 2014; Bhadra and Sarkar, 2009), which can dramatically enhance the mechanical strength and adhesion of PANI film. The effect of different sulphonic acid dopant types on morphological and electrical properties of PANI-PVA blend has already been reported (Bhadra et al., 2014). Self-assembly technique is well known in preparation of PANI-PVA nanorod and synthesis of PANI nanoparticles using DBSA as dopant and surfactant (Bhadra and Sarkar, 2009; Han et al., 2002). Therefore, we have chosen PVA to be the supporting polymer to overcome the shortcomings of pure PANI. In our present work, we have prepared PVA-PANI films doped with seven different monomer (aniline) concentrations. These films were prepared because the most desirable features of both conducting and conventional polymers can be combined synergistically. Although a great number of blends of PANI were investigated, much work remains to characterise the mechanical properties and its correlation with the electrical properties. In this context, we analyse and report the role of DBSA as dopant and surfactant; also we analyse the optimisation of aniline concentrations to achieve high conductivity and good mechanical strength.

2. Experimental details

This section describes the materials used and the methods adopted for characterisation of the polymer blends.

2.1. Materials

The ammonium persulphate (APS), DBSA and aniline used in the study were obtained from the Sigma Aldrich chemical company and were of very high purity (99.9%). PVA ($M_w = 31,000\text{--}50,000$) was also obtained from the Sigma Aldrich chemical company. The aniline was purified by repeated distillation under vacuum before its use. All other materials were used without any pre-processing.

2.2. Synthesis of PANI(DBSA)/PVA

Dispersion polymerisation is achieved using a technique described in the literature (Bhadra and Sarkar, 2009).

Polymerisation is initiated by adding ammonium persulphate drop-wise to the solution of aniline in aqueous PVA and DBSA under constant stirring. The bath temperature is maintained at 0–5 °C. After complete addition of the oxidant, the reaction is kept under constant stirring for 24 h. The reaction mixture becomes a bluish-green homogeneous mixture, indicating completion of the polymerisation reaction. Stand-alone films are prepared by casting the green suspension into a glass plate placed on a levelled flat surface for drying at room temperature. Table 1 describes the feeding ratio of aniline on the PANI-DBSA content of the PANI/DBSA-PVA blend.

2.3. Measurements

Scanning electron microscopy (SEM) is used to study the surface morphology and the grain size of the PANI in a nano-SEM Nova 450 apparatus. A Fourier-transform infrared spectrometer (FTIR) (8101 M, Shimadzu) is used to study the chemical interaction between the polymers. UV-Vis spectra are obtained with a PerkinElmer Lambda 15 spectrophotometer. To study the thermal properties of the PANI, thermogravimetric analysis (TGA) and differential scanning calorimetry (DSC) are performed with a PerkinElmer Pyris TGA and a PerkinElmer Precisely Jade DSC, respectively. Elemental analyses of the C, H and N atoms are performed in a PerkinElmer 2400 CHN Analyser. For the electrical measurements, thin films (40–60 μm) are prepared by spin coating the blend solution on a 2 cm × 2 cm preheated glass slide, and silver paste strips 1 mm wide and 1 cm long are formed on the films to be the contacts. The tensile properties are measured using an Instron 4465 (Canton, MA) universal testing machine. The mechanical properties are performed according to the ASTM-D882-12 standard with a crosshead speed of 50 mm/min at room temperature. At least five specimens are used for each test, with a gauge length of 25 mm, a width of 10 mm and a thickness of 1 mm. The electrical properties are studied by measuring the in-plane I - V characteristics and the four-probe conductivity using a Keithley 2400 source meter. A.C. electrical conductivity is conducted by using Novocontrol GmbH Concept 80 Broadband Dielectric Spectrometer for temperature range of 173–373 K.

3. Results and discussion

3.1. SEM images

Because SEM is a powerful magnification tool that utilises focused beams of electrons to obtain information, morphological investigations are performed using this approach to study the influence of the concentrations of aniline in the feed on the film morphology, as shown in Fig. 1. The SEM shows transformation of shapes from hexagonal (D_1) shape to near spherical (D_4) to hexagonal (D_7) again with different feeding ratios of aniline. PANI(DBSA)/PVA hexagonal flakes are about 250–300 nm thick of different sizes of few μm whereas for spherical particles are found to be 300–400 nm. This transition of different shapes with change in aniline concentration is clearly visible from SEM pictures. The transition is due to the change of micellar shape from hexagonal to spherical and again back to hexagonal with increase of aniline concentration. The increase in aniline concentration induces the change in molar ratio

Table 1 Weight contents used in the blend and PANI content calculated upon CHN elemental analyser.

Sample	PVA (gm)	DBSA (gm)	Aniline (gm)	PANI content in the blend (wt.%)	Type of film
PANI	0	1	0.25	100	Powder
PVA	2	0	0	–	Ductile
D ₁	2	1	0.25	0.65	Ductile
D ₂	2	1	0.50	2.44	Ductile
D ₃	2	1	0.75	4.71	Ductile
D ₄	2	1	1.00	5.92	Less ductile
D ₅	2	1	1.25	7.09	Brittle
D ₆	2	1	1.50	8.22	Very brittle
D ₇	2	1	1.75	9.65	Very brittle

between monomer and surfactant that causes the transition of micellar shape. A similar effect can also be observed in different attempts (Han et al., 2002; Thekkayil et al., 2014). The spherical particles of D₄ show uniform sized particles of nanometre dimension.

3.2. Infrared spectroscopy

The FTIR spectra (shown in Fig. 2) and their corresponding spectral peak assignments describe the effect of feeding ratio of aniline on chemical interactions of PANI(DBSA)/PVA blends. At the same time, FTIR spectra for pure PANI and PVA are also included as the inset of Fig. 2 for better comparison. The FTIR spectra of samples containing the blends indicate the presence and effect of variation in PANI content in the blends. The IR band at 3220–3185 cm⁻¹ is observed to have some red shift for NH stretch; with increase of PANI, the shift becomes more. Another band at 2910–2842 cm⁻¹ is assigned to C–H stretching due to the presence of methylene group in aliphatic backbones from PVA and hydrophobic tail in DBSA. This band is found to decrease with increase of PANI in the blend, which is obvious as PANI becomes the dominating species. Another absorption band at 1600–1560 cm⁻¹ is assigned to a benzenoid form C=C ring vibration. A vibrational stretch of a N-benzenoid ring can be seen at 1496–1493 cm⁻¹; the band at 1450–1461 cm⁻¹ is assigned to the C–N stretch of the quinoid ring, which is caused by protonation of PANI in PVA matrix by the dopants. The multiple peaks at 1191–1056 cm⁻¹ are found because of the absorption of sulphonic stretch of dopants. The presence of DBSA content is indicated by the presence of peaks 2910 cm⁻¹, 2846 cm⁻¹, 1320 cm⁻¹ and 1026 cm⁻¹ in all the blend samples. The peaks at 3220 cm⁻¹ and 1420 cm⁻¹ indicate the presence of PANI, exhibiting an increase in intensity with an increase in the PANI concentration (Li et al., 2008; Jin et al., 2010; Goel et al., 2007).

3.3. UV-Vis spectroscopy

UV-Vis spectroscopy is one technique used to study the electronic absorption of conducting polymers that is useful for investigating the oxidation and doping state of the polymer backbone. Pure PANI has two absorption peaks (shown in

inset of Fig. 3). The optical absorption spectra of the sulphonic acid-doped PANI–PVA blends are shown in Fig. 3, and peaks are listed in Table 2. As presented in Table 2, the absorption peaks for pure PANI exhibit two peaks at 274 nm and at 396 nm, whereas pure PVA only exhibits one absorption peak at 294 nm. In the sulphonic acid-doped PANI–PVA blends, the absorption peaks are observed at 290–276 nm and 438–420 nm, corresponding to the $\pi \rightarrow \pi^*$ of benzenoid rings and localised polarons (quinoid, Q), respectively. Another broad absorption peak is observed at 800 nm that is ascribed to an exciton located in the quinoid ring. This peak is evolved due to the charge transfer from adjacent benzenoid rings with each side contributing half electron on average (Yang et al., 2007). The height of this absorption peak provides information of the extent of doping level. The peak height is detected to increase until D₄, beyond that it is noticed to be same. That is why the order of conductivity also remains unchanged beyond D₄ (shown in Table 2). In other words, the dopant DBSA concentration remains same although aniline concentration is increased. Therefore, the dopant concentration in D₄ is sufficient for the available aniline. With increasing aniline concentration, both the peaks are found to have shifted from a higher wavelength to a lower wavelength. The increase in aniline quantity may have increased the compact coil conformation of the polymer leading to this blue shift.

3.4. Differential scanning calorimetry

DSC is most commonly used to determine the thermal transition temperatures, such as glass transitions, melting, cross-linking, and decomposition. However, DSC measures only the total heat flow and the sum of all thermal transitions in the sample. The DSC measurement of PANI/DBSA–PVA blends under a N₂ atmosphere is shown in Fig. 4 and summarised in Table 3, which reveals a broad endothermic peak in the range of 100–150 °C due to the elimination of water and impurities, which is also found in the TGA thermogram. The glass transition temperature of PANI is 80 °C. PANI/DBSA–PVA blends exhibit only a single glass transition temperature, which gradually decreases with increases in the PANI content in the blends until a PANI content of 6% is reached, and then starts to increase again with the PANI content. Generally, the shift trend of T_g can be considered as the index of miscibility of polymer blends.

3.5. Thermal gravimetric analysis

The TGA studies of the PANI(DBSA)/PVA blend films are performed in the range of 30–700 °C at a heating rate of 10 °C/min (as shown in Fig. 5 and summarised in Table 4) under an inert atmosphere. The TGA thermogram exhibits the following results: pure PVA, PANI and PANI(DBSA)/PVA blend exhibit weight loss in one step, three steps, and four steps, respectively. In pure PVA, the polymer backbone is stable up to 200 °C, with the polymer degradation commencing near 220 °C and completing at 320 °C. In the case of pure PANI and its blends, the 1st step of weight loss is found to be between 40 and 140 °C for PANI and between 40 and 110 °C for PANI(DBSA)/PVA blend; this first step of weight loss is caused by moisture, free acids and unreacted monomer, which are used as solvents and dopants in the preparation of the

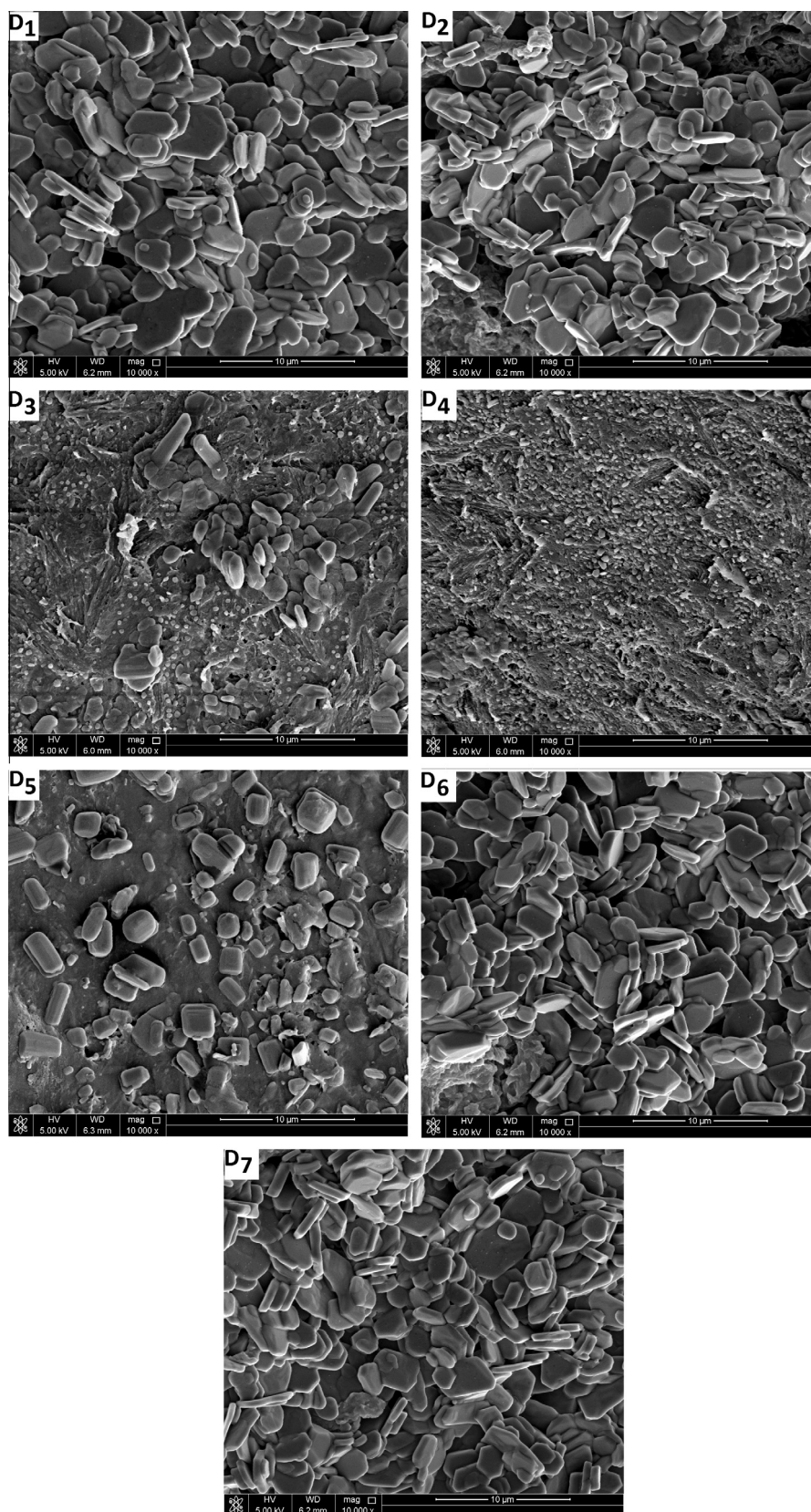


Figure 1 SEM images for seven concentrations of PANI: (a) D₁, (b) D₂, (c) D₃, (d) D₄, (e) D₅, (f) D₆, and (g) D₇.

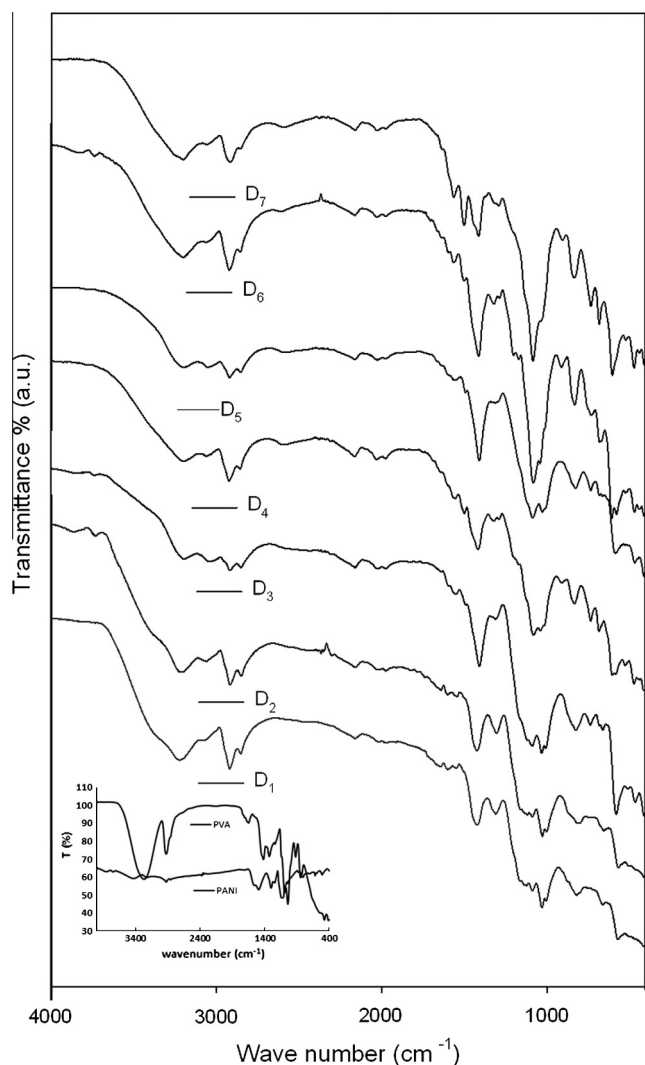


Figure 2 FTIR spectrum of the DBSA doped PANI-PVA blend. Inset: FTIR of pure PANI and PVA.

PANI. The major component of the volatiles in this step seems to be water molecules. The next step of weight loss in the range of 140–260 °C is observed only in the PANI(DBSA)/PVA blend films. This degradation step may be attributed to the short polymer or oligomer degradation produced during the polymerisation process (Pan et al., 2010; Babazadeh, 2009; Castillo-Castro et al., 2007). This peak temperature presented in Table 4 has an increasing trend with increases in PANI concentration. This is because with the increase in aniline concentration, the production of oligomer also increases. The next weight loss step for pure PANI and its blend films is found in the range 180–380 °C, which is caused by the degradation of Coulomb attraction between the sulphonic acid and PANI backbone ($\text{NH} + \dots \text{SO}^{-3}$ interaction between the PANI chain and DBSA dopant), because the acid itself begins to evaporate and degrade (Hosseini and Entezami, 2001). Furthermore, the molecular interaction (e.g., hydrogen bonding) amongst the acid, PVA and PANI is no longer effective at this stage; therefore, a major weight loss takes place. With increase in PANI concentration, this peak temperature increases due to increase in number of interaction sites between PANI chain

and DBSA dopant. The fourth and final weight loss step lies in the range between 380 and 480 °C (Basavaraja et al., 2009; Hosseini and Entezami, 2005), as presented in Table 4. The final degradation temperatures for all of the blends are higher than those of the constituent polymers (PANI and PVA). The 3rd and 4th degradation temperatures are found to increase from D_1 to D_4 and then to decrease; these results indicate that the blending process increases the stability of the polymer blend until D_4 . In all cases, the final residue after TGA is approximately 30% of the weight. This result indicates that each blend forms a similar residue irrespective of the PANI content. The PANI-DBSA salts were not completely destroyed, because in nitrogen atmosphere, carbonisation of polymer takes place leaving a marked residue.

3.6. Mechanical properties

The tensile strength and elongation at break of the PANI(DBSA)/PVA blend films are investigated and plotted as a function of PANI wt% (shown in Fig. 6). From Fig. 6, it is evident that the tensile strength depends strongly on the PANI content. Because PANI is known to be a very rigid material, the tensile strength of the PANI blends was maintained as the concentration of PANI increased up to 5%. With over 5% of PANI, the rigid or brittle characteristics of

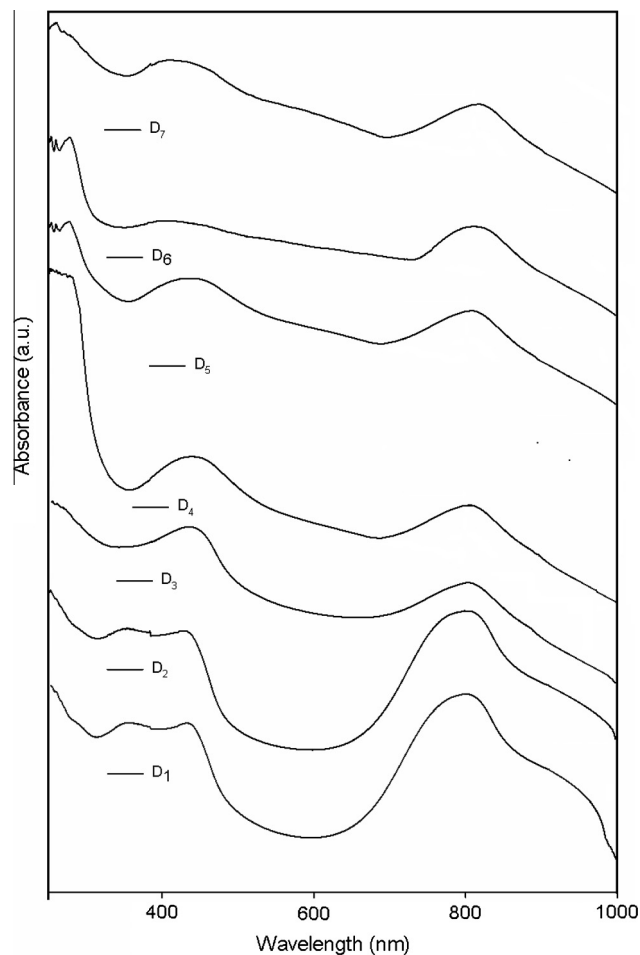


Figure 3 UV-Vis spectrum of the DBSA doped PANI-PVA blend. Inset: UV-Vis absorption spectrum of pure PANI.

Table 2 Table tensile strength, UV–Vis peak positions and conductivity of PANI, PVA and seven DBSA doped PANI–PVA blend films.

Polymer	Tensile strength (MPa)	UV–Vis peaks (nm)	Conductivity (S/cm)
PANI	–	274, 396	8.4×10^{-2}
PVA	26.963	294	7.9×10^{-13}
D ₁	0.18273	290, 438	1.2×10^{-8}
D ₂	0.25738	289, 434	2.8×10^{-4}
D ₃	0.26789	286, 433	5.01×10^{-3}
D ₄	1.6840	283, 432	1.1×10^{-2}
D ₅	0.60216	277, 431	1.8×10^{-2}
D ₆	0.58800	276, 421	2.5×10^{-2}
D ₇	0.64453	276, 420	2.5×10^{-2}

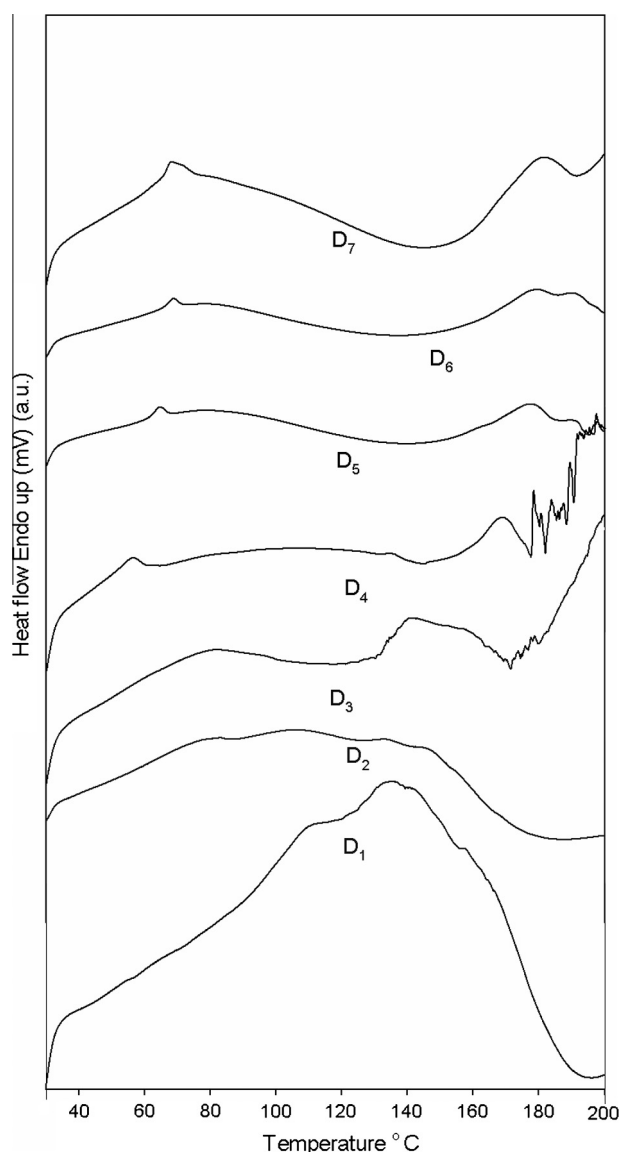


Figure 4 DSC of the DBSA doped PANI–PVA blend.

pristine PANI become dominant; as a result, above 5% of PANI the tensile strength of the PANI blend decreases substantially. The reason for this behaviour might be that at a

PANI content less than 5%, the PANI is dispersed in the form of separate islands in the PVA matrix, thereby enhancing the strength of the blend. Beyond this concentration of 5% PANI, the PANI forms globular aggregates in the matrix, thus reducing the tensile strength (Jeevananda and Siddaramaiah, 2003; Soares and Leyva, 2007). However, the elongation of the blend films, decreases steadily with increases in the PANI content in the blend because of the rigid or brittle nature of PANI.

3.7. Electrical properties

3.7.1. D.C. conductivity

Fig. 8 represents the conductivity of the PANI(DBSA)/PVA blend films as a function of the PANI content. The electrical conductivity of the blend films depended strongly on the weight fraction of PANI in the blends (Ikkalaa et al., 1995). Additionally, as shown in the figure, the PANI(DBSA)/PVA blends were percolating systems. The scaling law of percolation theory (Banerjee and Mandal, 1995) can be applied to the data presented in Fig. 7:

$$\sigma = c(f - f_p)^t \quad (1)$$

where c is a constant, t is a critical exponent, and σ is the electrical conductivity. f and f_p represent the PANI weight fraction in the composites and the PANI weight fraction at the percolation threshold, respectively. The percolation threshold was determined to be 0.79 wt%, which was calculated from fitting the experimental data using a plot of $\log \sigma$ vs. $\log (f - f_p)$. The fit had a very good correlation ($R^2 = 0.99$), and the value of the exponent t is 2.1, which represents two-dimensional conductivity. As stated above, the network of globular aggregates of PANI is formed at PANI concentrations above 5%. This network of globular aggregates of PANI is responsible for the constant trend of conductivity above 5% PANI, which is consistent with the saturation observed in the data of the mechanical properties previously discussed. The conductivity achieved for the PANI blend containing 5% PANI (10^{-2} S/cm) is well above those reported in the literature, 10^{-6} and 10^{-7} S/cm, for samples containing the same amount of PANI. Thus, *in situ* polymerisation is an effective method for producing polymer blends of higher electrical conductivity and lower percolation thresholds that are achievable via the use of conducting polymers with fillers. Therefore, the relatively low percolation threshold indicated that the two classes of polymers (PANI and PVA) had interactions and good miscibility.

Table 3 Table containing DSC melting temperature of PANI, PVA and seven DBSA doped PANI–PVA blends.

Polymers	T_g (°C)	T (°C)
PANI	80	130
PVA	–	220
D ₁	98	132
D ₂	83	133
D ₃	80	140
D ₄	56	167
D ₅	64	177
D ₆	68	178
D ₇	70	182

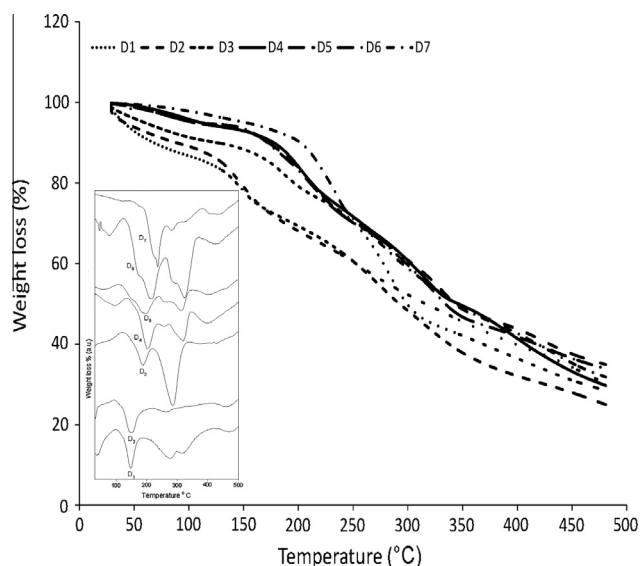


Figure 5 TGA of the DBSA doped PANI-PVA blend. Inset: DTA curve of DBSA doped PANI-PVA blend.

Table 4 Table containing TGA degradation temperature of PANI, PVA and seven DBSA doped PANI-PVA blends.

Polymer	No of degradation steps	Peak degradation temperature			
		1st step	2nd step	3rd step	4th step
PANI	3	100	–	280	480
PVA	1	–	–	278	–
D ₁	4	60	146	275	465
D ₂	4	70	148	266	457
D ₃	4	90	185	284	425
D ₄	4	88	186	316	510
D ₅	4	75	214	332	500
D ₆	4	73	209	322	498
D ₇	4	60	233	318	495

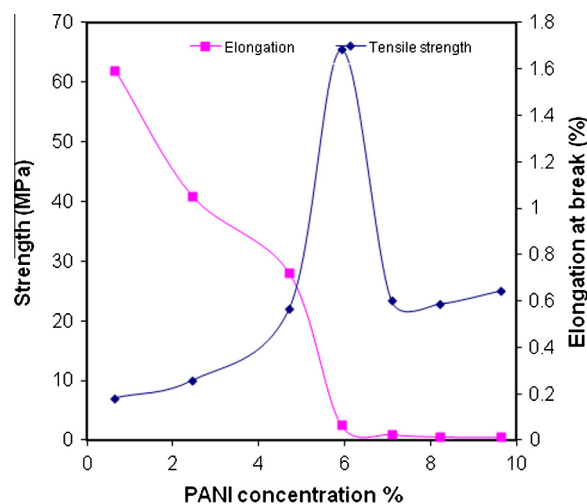


Figure 6 Tensile strength and % elongation of PANI(DBSA)/PVA versus the weight percentage of aniline.

3.7.2. A.C. conductivity

The basis electrical conductivity in the conducting polymers is mainly due to the movement of delocalised electrons through the polymer backbone systems and at the same time hopping of electrons between the nearest neighbour redox sites on the polymer chain. The frequency dependent conductivity ($\sigma(f)$) of PANI(DBSA)/PVA systems for two temperatures is shown in Fig. 8. Almost similar trends in the $\sigma(f)$ are seen for all the blend samples, except there is a significant increase in conductivity values with increase in aniline concentration in the blend. For low temperature 200 K for all the blend samples there was no change in the $\sigma(f)$ up to 10^2 Hz, and a rapid increase is observed after this frequency. This rapid increase in $\sigma(f)$ is due to increase in hopping of the electrons at relatively high frequencies. Similar trends are observed for all the blends; however, beyond the frequency 10^6 Hz the increase seen in the $\sigma(f)$ became slower. The frequency dependent conductivity at room temperature 300 K shows increase in $\sigma(f)$ with frequency, without any significant changes unlike at low

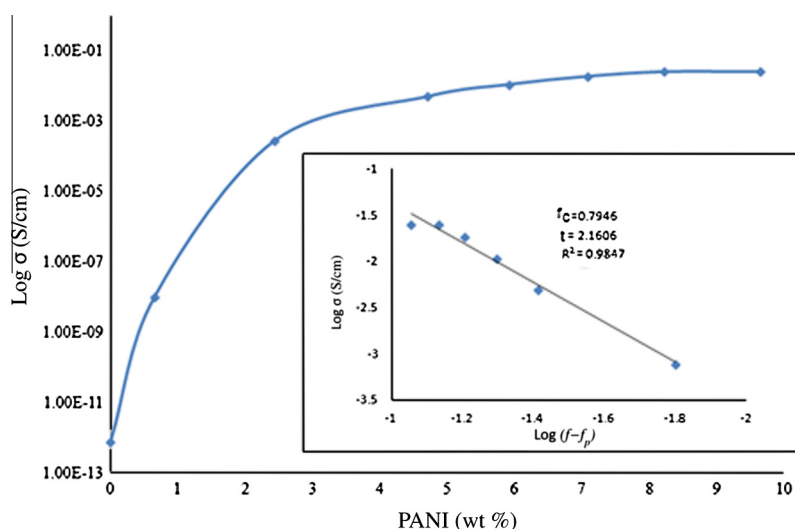


Figure 7 Electrical conductivity as a function of aniline content (doped with DBSA) in PANI blends with PVA.

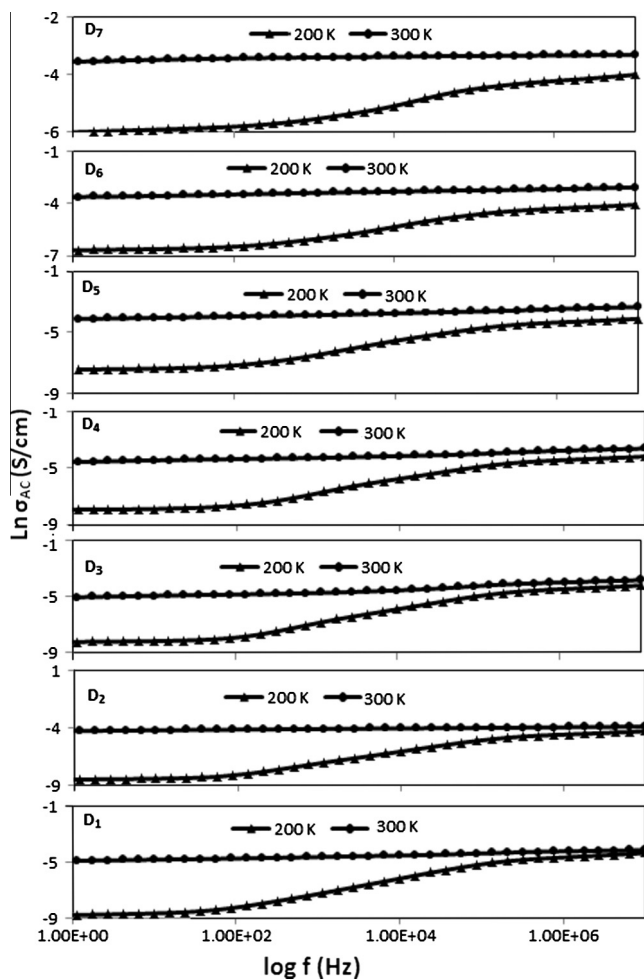


Figure 8 Frequency dependence of A.C. conductivity for PANI(DBSA)/PVA blends at two different temperatures.

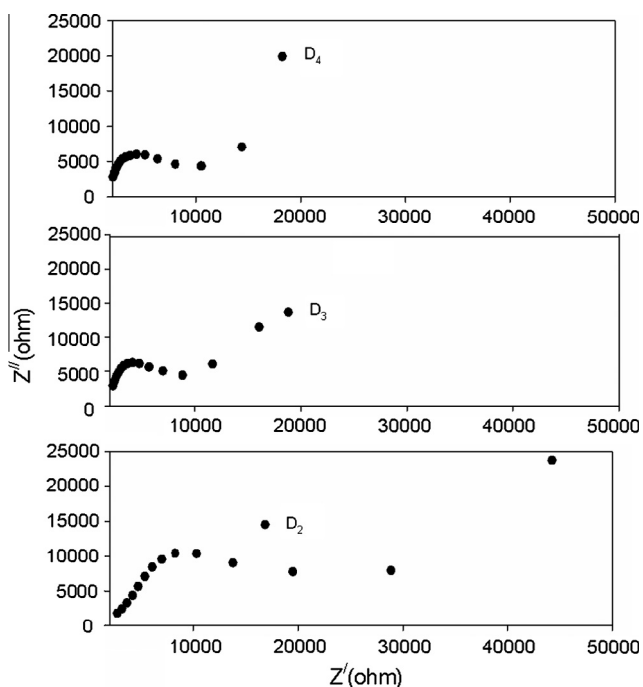


Figure 9 Nyquist plot for D₂–D₄ at room temperature.

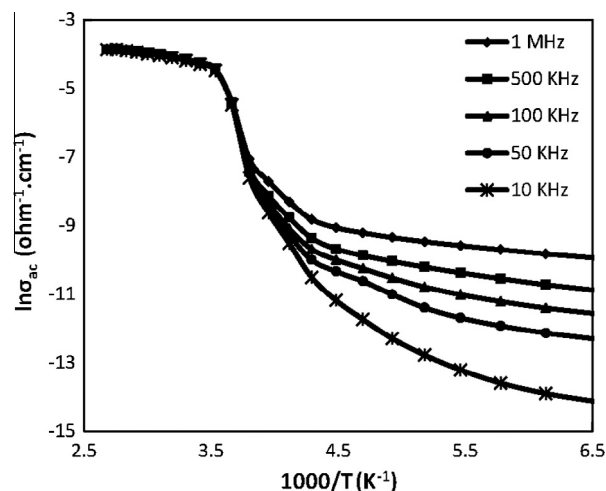


Figure 10 Effect of temperature on A.C. conductivity for PANI(DBSA)/PVA blend for D₄.

temperature. In both types of motions, i.e., charge carriers through the polymer backbone system and hopping of electron between localised sites can be affected by the frequency and also the aniline concentration positively.

The Cole–Cole or Nyquist plot of the complex impedance $Z = Z' + Z''$, (Real (Z) versus Im (Z)) at room temperature for D₂–D₄ is shown in Fig. 9 for frequency range of 50 kHz to 1 MHz. Theoretically, an ideal Nyquist impedance plot features a semicircle over the high frequency region and a linear part in the low frequency range. The plot for three PANI(DBSA)/PVA blends shows similar trend like ideal Nyquist impedance plot. The D₂ blend with low aniline content has the larger semicircle amongst the three, which represents higher interfacial charge-transfer resistance and is attributed to the poor electrical conductivity of the materials, whereas D₄ has the smallest radius of semicircle indicating low resistance and high conductivity of the material. And the straight line of the Nyquist plot in the lower frequency region corresponds to the resistance resulting from ion diffusion.

The temperature dependent conductivity for sample D₄ for five different frequencies conducted is shown in Fig. 10. From the plot it is seen that at high temperature region for all frequencies there is no change in conductivity. However the difference in the conductivity values can be seen in low temperature region. From the plot it is also clear that the mode of conductivity is different for low temperature and high temperature for all the frequency ranges.

4. Conclusions

In this experiment, optimisation of the aniline was performed to obtain a free-standing PANI(DBSA)/PVA film for use in various semiconductor applications. The systematic study was conducted for morphology, thermal, mechanical and most importantly electrical conductivity. The shape of PANI(DBSA)/PVA particles shows variation from hexagonal (D₁) to spherical (D₄) and then to hexagonal (D₇) that is due to the change of micellar shape, i.e. from hexagonal to spherical and again back to hexagonal, with increase in aniline concentration. FTIR spectra show shift of peaks at 3220 cm⁻¹ and

1420 cm^{-1} from higher wavelength to a lower wavelength, indicating the increase of PANI concentration in the blends. The major degradation peak of TGA thermogram increases with increase in PANI concentration indicating increase in stability because of the raise in number of $\text{NH} + \cdots \text{SO}^{-3}$ interaction between PANI chain and DBSA dopant. PANI/DBSA-PVA blends exhibit only a single glass transition temperature, which gradually decreases with increase in PANI content in the blends until a PANI content of 6% is reached. Thereafter it starts to increase again with the PANI content. The study of tensile property shows that elongation of the blend films decreases steadily with increase in PANI content in the blend because of the rigid or brittle nature of PANI. We carefully followed the standard protocol during this study and achieved a conductivity of the blends in the range of 10^{-4} to 10^{-2} S/cm and the percolation threshold ≈ 0.79 wt% PANI. In other words, a higher conductivity and lower percolation threshold were obtained compared with the values reported in the literature. Frequency dependent A.C. conductivity indicates that the mode of conductivity for all the frequencies is different for different temperature spectrum, i.e. low, high, etc. Thus we believe that PANI(DBSA)/PVA blends could find potential applications, especially in flexible electronic devices, due to their excellent electrical and mechanical properties.

References

- Afzal, A.B., Akhtar, M.J., Ahmad, M., 2010. Morphological studies of DBSA-doped polyaniline/PVC blends. *J. Electron Mic.* 59, 339–344.
- Araujo, P.L.B., Aquino, K.A.S., Araujo, E.S., 2007. Effects of gamma irradiation on PMMA/polyaniline nanofiber composites. *Int. J. Low Radiat.* 4, 149–160.
- Babazadeh, M., 2009. Aqueous dispersions of DBSA-doped polyaniline: one-pot preparation, characterization, and properties study. *J. Appl. Polym. Sci.* 113, 3980–3984.
- Banerjee, P., Mandal, B.M., 1995. Conducting polyaniline nanoparticle blends with extremely low percolation thresholds. *Macromolecules* 28, 3940–3943.
- Basavaraja, C., Kim, N.R., Jo, E.A., Pierson, R., Huh, D.S., Venkataraman, A., 2009. Transport properties of polypyrrole films doped with sulphonic acids. *Bull. Korean Chem. Soc.* 30, 2701–2706.
- Bhadra, J., Sarkar, D., 2009. Self-assembled polyaniline nanorods synthesized by facile route of dispersion polymerization. *Mater. Lett.* 63, 69–71.
- Bhadra, J., Madi, N.K., Al-Thani, N.J., Al-Maadeed, M.A., 2014. Polyaniline/polyvinyl alcohol blends: effect of sulfonic acid dopants on microstructural, optical, thermal and electrical properties. *Synth. Met.* 191, 126–134.
- Castillo-Castro, T.D., Castillo-Ortega, M.M., Villarreal, I., Brown, F., Grijalva, H., Pérez-Tello, M., Nuño-Donlucas, S.M., Puig, J.E., 2007. Synthesis and characterization of composites of DBSA-doped polyaniline and polystyrene-based ionomers. *Composites: Part A* 38, 639–645.
- Goel, S., Gupta, A., Singh, K.P., Mehrotra, R., Kandpal, H.C., 2007. Optical studies of polyaniline nanostructures. *Mater. Sci. Eng., A* 443, 71–76.
- Han, M.G., Cho, S.K., Oh, S.G., Im, S.S., 2002. Preparation and characterization of polyaniline nanoparticles synthesized from DBSA micellar solution. *Synth. Met.* 103, 3415–3422.
- Hopkins, A.R., Tomczak, S.J., Vij, V., Jackson, A.J., 2011. Small Angle Neutron Scattering (SANS) characterization of electrically conducting polyaniline nanofiber/polyimide nanocomposites. *Thin Solid Films* 520, 1617–1620.
- Hosseini, S.H., Entezami, A.A., 2001. Preparation and characterization of polyaniline blends with polyvinyl acetate, polystyrene, and polyvinyl chloride for toxic gas sensors. *Polym. Adv. Technol.* 12, 482–493.
- Hosseini, S.H., Entezami, A.A., 2005. Studies of thermal and electrical conductivity behaviours of polyaniline and polypyrrole blends with polyvinyl acetate, polystyrene and polyvinyl chloride. *Iran. Polym. J.* 14, 201–209.
- Ikkalaa, O.T., Lindholm, T.M., Ruohonenc, H., Selantaub, M., Vakipartac, K., 1995. Phase behavior of polyaniline/dodecyl benzene sulphonic acid mixture. *Synth. Metal.* 69, 135–136.
- Jeevananda, T., Siddaramaiah, 2003. Synthesis and characterization of polyaniline filled PU/PMMA interpenetrating polymer networks. *Eur. Polym. J.* 39, 569–578.
- Jin, E., Bian, X., Lu, X., Kong, L., Wang, C., Zhang, W., 2010. Facile synthesis of polyaniline derivatives hollow microspheres with porous shells deposited on glass substrate. *Mater. Chem. Phys.* 120, 336–340.
- Kim, S.H., Oh, K.W., Kim, T.K., 2005. Novel conducting polyaniline blends with cyanoresin. *J. Appl. Polym. Sci.* 96, 1035–1042.
- Li, G., Zhang, C., Peng, H., 2008. Facile synthesis of self-assembled polyaniline nanodisks. *Macromol. Rapid Commun.* 29, 63–67.
- Malmonge, L.F., Langiano, S.C., Cordeiro, J.M.M., Mattoso, L.H.C., Malmonge, J.A., 2010. Thermal and mechanical properties of PVDF/PANI blends. *Mater. Res.* 13, 465–470.
- Morita, M.J., 1994. Effects of solvent and electrolyte on the electrochromic behavior and degradation of chemically prepared polyaniline-poly(vinyl alcohol) composite films. *Polym. Sci. Pt. B: Polym. Phys.* 32, 231–242.
- Pan, W., Qu, L., Chen, Y., 2010. Conductive blends of dodecylbenzene sulfonic acid-doped polyaniline with poly (vinyl pyrrolidone). *Optoelectron. Adv. Mat. – Rapid Commun.* 4, 2123–2128.
- Pawar, P.A., Purwar, A.H., 2013. Biodegradable polymers in food packaging. *Am. J. Eng. Res.* 2, 151–164.
- Soares, B.G., Leyva, M.E., 2007. Effect of blend preparation on electrical, dielectric, and dynamical-mechanical properties of conducting polymer blend: SBS triblock copolymer/polyaniline. *Macromol. Mater. Eng.* 292, 354–361.
- Thekkayil, R., Philip, R., Gopinath, P., John, H., 2014. Energy dependent saturable and reverse saturable absorption in cube-like polyaniline/polymethyl methacrylate film. *Mater. Chem. Phys.* 146, 218–223.
- Wu, G., Zhang, H., 2013. Synthesis and characterization of camphor sulfonic acid fully doped polyaniline. *RAM* 1, 5–8.
- Yang, Y., Ding, Y., Chen, G., Li, C., 2007. Synthesis of conducting polyaniline using novel anionic Gemini surfactant as micellar stabilizer. *Eur. Polym. J.* 43, 3337–3343.
- Yuxi, Z., Rutledge, G.C., 2012. Electrical conductivity of electrospun polyaniline and polyaniline-blend fibers and mats. *Macromolecules* 45, 4238–4246.
- Zareh, E.N., Moghadam, P.N., Azariyan, E., Sharifian, I., 2011. Conductive and biodegradable polyaniline/starch blends and their composites with polystyrene. *Iran. Polym. J.* 20, 319–328.